Scientific Research

Thermal and Structural Analyses of PMMA/TiO₂ Nanoparticles Composites

Nabawia A. El-Zaher¹, Mohamed S. Melegy², Osiris W. Guirguis²

¹Textile Metrology Lab, National Institute for Standards, Giza, Egypt
²Biophysics Department, Faculty of Science, Cairo University, Giza, Egypt
Email: nabawia@yahoo.com, ms_melegy@hotmail.com, osiris_wgr@yahoo.com

Abstract

In the present work, composites of poly(methyl methacrylate)/titanium oxide nanoparticles (100/0, 97.5/2.5, 95/5, 92.5/7.5, 90/10 and 0/100 wt/wt%) were prepared to be used as bio-equivalent materials according to their importance broad practical and medical applications. Thermal properties as well as X-ray diffraction analyses were employed to characterize the structure properties of such composite. The obtained results showed variations in the glass transition temperature (T_g), the melting temperature (T_m), shape and area of thermal peaks which were attributed to the different degrees of crystallinity and the existence of interactions between PMMA and TiO₂ nanoparticle molecules. The XRD patterns showed sharpening of peaks at different concentrations of nano-TiO₂ powder with PMMA. This indicated changes in the crystallinity/amorphosity ratio, and also suggested that the miscibility between the amorphous components of homo-polymers PMMA and nano-TiO₂ powder is possible. The results showed that nano-TiO₂ powder mix with PMMA can improve the thermal stability of the homo-polymer under investigation, leading to interesting technological applications.

Keywords

1. Introduction

Polymeric materials have special interest because in combination with suitable metal salts, they give complexes which are useful for the development of advanced high energy electrochemical devices and photo electro-

chemical cells with ease of fabrication into thin films of desirable sizes. Also, an exponential growth of research activities has been seen in nanoscience and nanotechnology in the past decades [1] [2]. New physical and chemical properties emerge when the size of the material becomes smaller and smaller, and down to the nanometer scale. Fillers are used in polymers for variety of reasons: cost reduction, improved processing, density control, optical effect, thermal conductivity, control of thermal expansion, electrical properties, magnetic properties, flame retarding and hardness, etc. [3].

Polymer-inorganic oxide nanoparticle composites have attracted considerable attention in the field of material science because they exhibit enhanced material properties as compared to pure polymers. The presence of inorganic oxide nanoparticle fillers in polymers can alter the thermomechanical, optical, electrical, and magnetic properties of the polymers [4]. Recently, composite materials made of polymers and nanoparticles (NPs), such as inorganic, metal, semiconductor, carbon black, and magnetic nanomaterials have attracted great attention because of the stabilizing effects of the polymer matrix on the NPs and relative easiness and flexibility of engineering this class of materials with advanced functionalities [4]-[9].

Poly(methyl methacrylate) (PMMA) is an important thermoplastic material, and its wide applications in many technological and productive fields take advantages of the unique combination of excellent optical properties (clarity, transparency from the near ultraviolet to the near infrared), with chemical inertness, some good mechanical properties, thermal stability, electrical properties, safety, weather resistance, model ability and easy shaping [10]. In addition, PMMA is one of the best organic optical materials which is very suitable for numerous imaging and non-imaging microelectronic applications, including as a photoresistance for direct-write e-beams, X-rays and deep UV microlithographic process and has been widely used to make a variety of optical devices, such as optical lenses either in the pure or doped state [11] [12]. PMMA has been used in skeletal surgery for more than 40 years as a means of securing prosthetic implants and more recently is used as a delivery agent for local high-dose antibiotics to treat soft tissue and osseous infections [13] and it has been extremely utilized for antibiotic delivery system purposes for the treatment of osteomyelitis [14]. Also, PMMA is a widely used support medium for the embedding of intact, undecalcified bone [15]. Its hardness makes it ideal for calcified tissue sectioning and subsequent histological examination [16].

In the early twentieth century, titanium dioxide (TiO_2) has been widely used as a pigment1 and in sunscreens, 2, 3 paints, 4 ointments, toothpaste, 5 etc. [17]. Moreover, enormous efforts have been devoted to the research of TiO_2 material, which has led to many promising applications in areas ranging from photovoltaics and photocatalysis to photo-/electro-chromics and sensors [18]. These applications can be roughly divided into "energy" and "environmental" categories, many of which depend not only on the properties of the TiO_2 material itself but also on the modifications of the TiO_2 material host (e.g., with inorganic and organic dyes) and on the interactions of TiO_2 materials with the environment. Also, titanium oxide (TiO_2) nanoparticle has been used in purification of polluted air and waste waters [19]. On other hand, nano-TiO_2 is not inert and is a UV light attenuator; therefore, it finds applications as a catalyst and as a UV light attenuator as opposed to a visible light attenuator [17]. Nano-TiO_2 is used as a UV stabilizer or blocker in products other than sunscreens, such as plastic products and textiles. Nano-TiO_2 protects both the matrix and the material behind the matrix from degradation due to UV light [20].

Chen *et al.* [21] reported in their study the synthesis and characterization of trialkoxysilane-capped poly-(methyl methacrylate)-titania hybrid optical thin films. The effect of shape and surface chemistry of TiO_2 colloidal nanocrystals on the organic vapor absorption capacity of TiO_2/PMMA composite is studied by Convertino *et al.* [22]. Osiris *et al.* [23] studied the macrostructure and optical properties of PMMA/TiO_2 nanoparticles composites.

In the present work, PMMA is mixed with different concentrations (2.5, 5, 7.5, and 10 wt%) of nano-TiO_2 powder. Thermal analyses [differential scanning calorimetry (DSC) and thermogravimetric analysis (TGA)] as well as X-ray diffraction (XRD) techniques are employed to characterize and to reveal the relationship of the structure properties of PMMA to be used in different technological applications.

2. Experimental Setup

2.1. Materials and Sample Preparation

For the present work, poly(methyl methacrylate) powder of chemical formula $[CH_2C(CH_3)(CO_2CH_3)-]_n$ with average molecular weight of 320,000 and melting point >150°C is supplied from Alfa Aesar, GmbH & Co., UK.

Furthermore, titanium (IV) oxide nanopowder as a mixture of rutile and anatase, with particle size less than 100 nm (BET) with 99.5% trace metals basis is supplied from Sigma-Aldrich, China.

The PMMA powder is mixed with nano-TiO_2 powder for four different concentrations (2.5, 5, 7.5 and 10 wt%). The starting materials are grounded using a Phillips PW 4018/00 Mini-Mill for 15 minutes with a rotating speed of 3400 rpm to form a homogeneous mixture as previously reported and checked [23].

2.2. Thermogravimetric Analysis (TGA)

Thermal behaviour of the prepared samples is examined by Thermogravimetric Analyzer model Schimadzu TGA-50H (Kyoto, Japan) from 25˚C to 600˚C. A heating rate of 10˚C/minute is used under nitrogen atmosphere and at a flow rate of 30 mL/minute. Dry sample weighing about 6.9012 mg is used. The standard uncertainty of the sample mass measurement is ±1%. The instrument is calibrated using calcium oxalate which was supplied along the instrument.

2.3. Differential Scanning Calorimetry (DSC)

The thermal transition behaviour of the prepared samples is determined by Differential Scanning Calorimeter model Schimadzu DSC-50 (Kyoto, Japan) from 25˚C to 600˚C. A heating rate of 10˚C/minute is used under nitrogen atmosphere and at a flow rate of 20 mL/minute. The sample weight was about 7.7167 mg.

2.4. X-Ray Diffraction (XRD)

The X-ray diffraction (XRD) measurements of the prepared samples are recorded with a Scintag Irc X-Ray Diffractometer (USA) equipped with Ni-filtered CuK_α radiation (λ = 1.5418 Å) and operated at 45 kV and 40 mA. The diffractograms are recorded in the range of 2θ from 5˚ to 60˚ at a speed rate of 2 degrees/minute. The crystallinity index (CrI) is calculated for the different samples using the relation [24]:

$$CrI = \left[\left(I_f - I_s \right) / I_f \right] \times 100 \tag{1}$$

where I_f is the peak intensity of the fundamental band at 2θ = 13.5˚ - 14.8˚ and I_s is the peak intensity of the secondary band at 2θ = 30.0˚ - 31.0˚. The CrI is a time-save empirical measure of relative crystallinity.

3. Results and Discussion

3.1. Thermal Gravimetric Analysis (TGA)

Thermal gravimetric analysis (TGA) is widely used to investigate the thermal decomposition of polymers to determine the thermal decomposition kinetic parameters such as activation energy and reaction order. These parameters can be used to obtain a better understanding of thermal stability of polymers. Also, TGA enables to determine a value of moisture loss of the polymers in addition to that obtained by conventional methods.

The TGA curves for pure PMMA, pure TiO_2 and that for PMMA mixed with 2.5, 5, 7.5 and 10 wt% nano-TiO_2 samples are shown in **Figure 1**. The kinetic parameters obtained from these curves are listed in **Table 1**. It is clear from the figure that, the curves show four weight loss steps and discuss as follows: The weight loss in the first step corresponds to the evaporation of bound water (desorption of water physically bound to the polymer and dehydration of it). This produces a broad not sharp endothermic peak which ends at around 90˚C - 100˚C. So, an initial weight resulting from moisture departing appeared starting from room temperature up to around 100˚C. It is well known that the melting temperature of a polymer decreases with increasing moisture content [25]. The lower values of % weight loss in the first step affirm the presence of a thermal process due to moisture evaporation from samples and also may be due to splitting or volatilization of small molecules and/or monomers in which weight loss varies between 0.36% and 6.396% and begins at near 40˚C. This lower value of weight loss enables one to suggest that the transitions observed in the corresponding temperature range of the following DSC spectra explain the existence of physical transition [26]. From **Table 1(a)**, it is noticed that, the first step mid-point temperature of the PMMA/TiO_2 nanoparticles composites are higher than that of the pure PMMA and in between the mid-point temperatures of the pure PMMA and pure nano-TiO_2 powder (an increase of about 6.1% for the composite 95/5 wt/wt% is detected). By following the % weight loss occurred in the first step, composites 97.5/2.5 and 95/5 wt/wt% lost a quantity from their weights less than that of the pure PMMA

Table 1. TGA and DrTGA data for PMMA/TiO$_2$ nanoparticles composites.

(a)

PMMA/TiO$_2$ (wt/wt%)	First step		Second step		Third step		Fourth step	
	% weight loss	Mid point (°C)	% weight loss	Mid point (°C)	% weight loss	Mid point (°C)	% weight loss	Mid point (°C)
100/0	0.664	44.92	37.860	271.86	56.790	325.00	0.168	393.00
97.5/2.5	0.368	52.77	33.805	268.22	53.731	345.51	7.846	388.00
95/5	0.391	47.68	17.768	255.88	67.839	325.90	4.091	391.23
92.5/7.5	2.342 1.491	44.62 89.76	31.303	267.68	51.448	343.15	1.301	392.58
90/10	6.396 3.315	45.86 93.63	26.731	269.09	49.145	348.68	2.044	393.94
0/100	8.916	64.18	2.633	215.60				

(b)

PMMA/TiO$_2$ (wt/wt%)	Total % weight loss	Residue %
100/0	95.482	4.518
97.5/2.5	95.750	4.250
95/5	90.089	9.911
92.5/7.5	87.885	12.115
90/10	87.631	12.369
0/100	11.549	88.451
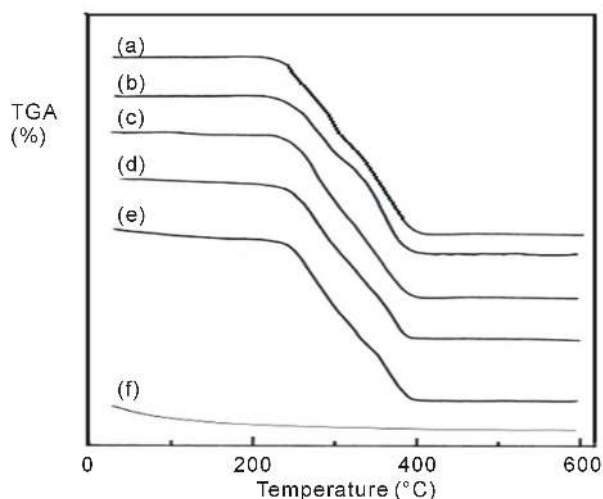
Figure 1. TGA curves of PMMA/TiO$_2$ nanoparticles composites: (a) 100/0, (b) 97.5/2.5, (c) 95/5, (d) 92.5/7.5, (e) 90/10 and (f) 0/100 (wt/wt%).

by about 45% and 41%, respectively, while composites 92.5/7.5 and 90/10 wt/wt% lost a quantity from their weight higher than that of the pure PMMA by about 124.6% and 399.4%, respectively. The percentage weight loss for pure TiO$_2$ is about 3.92% of its starting weight and its mid-point occurs at about 64.18°C. It is also noticed from the table for composites 92.5/7.5 and 90/10 wt/wt% that, another loss in their weights occurred and their mid-point temperatures located at about 89.8°C and 93.6°C.

The second loss peak starting at above 200°C (see **Figure 1**) is ascribed to crystal cleavage (most clearly in the pure PMMA) and may be attributed to melting and degradation of different morphological components forming the highly complex structure of PMMA. It is characterized by the presence of the typical melting endotherm with a single peak at 271.86°C. This second step corresponds to the weight loss caused by the decomposi-

tion of the PMMA structure, and coincides with the temperature range over which a number of defined paralysis reactions takes place in PMMA [10]. The hydrogen bond of methyl group ruptures and ordered regions of PMMA undergo a solid to liquid phase change. The initial temperature of the thermal decomposition stage is usually used to compare the thermal stability of the samples which is in agreement with that previously reported [27] [28]. Chiu [27] reported that the temperature at which mass loss starts and proceeds at its fastest rate is unique for any given polymer and the technique can be used for characterization purposes.

Furthermore, it is noticed that, the second step mid-point temperature of the PMMA/TiO$_2$ nanoparticles composites are smaller than that of the pure PMMA and in between the mid-point temperatures of the pure PMMA and pure nano-TiO$_2$ powder (a lowest decrease of about 5.9% for the composite 95/5 wt/wt% is detected). By following the % weight loss occurred in the second step, the lowest % weight loss is occurred for composite 95/5 wt/wt% than that of the pure PMMA sample and is about 53.1%. For the third step the decomposition of 97.5/2.5, 92.5/7.5 and 90/10 PMMA/TiO$_2$ nanoparticles composites occurs at about 343°C - 348°C and they are higher than that of the pure PMMA. For composite 95/5 the decomposition mid-point temperature was about at 325.90°C which is approximately the same as the pure PMMA (325°C), also, this composite shows the highest % weight loss and greater than that of the pure PMMA sample (about 19.5%). The lowest value in % weight loss smaller than that of the pure PMMA sample is detected for composition 90/10 wt/wt% and is about 15.6%. Another decomposition stage (fourth step) is detected and the decomposition midpoint temperature was nearly the same as the pure PMMA (393°C). A non-remarkable decrease of about 1.3% for the composite 97.5/2.5 wt/wt% is detected and the composites loose their weight by increasing the nano-TiO$_2$ powder.

From **Table 1(b)**, at the end of the thermal degradation of the PMMA/TiO$_2$ nanoparticles composites, it is indicated that, the total % weight loss decreases by increasing the concentration of nano-TiO$_2$ in the composite till 10 wt% of TiO$_2$ (about 8.2%), *i.e.* the char residue for this composite is the highest one (12.369)—Char weight = W$_1$ – W$_2$; where W$_1$ is the total weight of the composite at the starting thermal process and W$_2$ is the total weight loss of the composite at the end process—so, the production of more char (less in weight loss during the composition) in case of PMMA mixed with nano-TiO$_2$ at concentration of 10 wt% means that thermal stability of this sample is enhanced and it is more resistant to fire hazards. When the temperature rises above 300°C; slight final loss occurs, this is caused by the chemical groups in the crystalline regions of the polymer. Therefore, following the rise in temperature, PMMA polymer first decomposes in the amorphous region, and then in the crystalline region. Thermal degradation of PMMA sequently occurs as initial scission, depropagation reactions and further degradation into volatile compounds [29].

At least two mechanisms have been validated for the initial scission of PMMA, including random scission (C-C bonds) of the main chain and hemolytic scission of the methoxycarbonyl side groups (-COOCH$_3$). The random C-C scission is the dominant mechanism, which decomposes PMMA into methyl methacrylate as a major product [30]. However, the products such as CO$_2$, CO, CH$_3$OH, CH$_4$ and char, other than the monomer could also form along with the elimination of methoxycarbonyl side groups [31]. The kinetics of PMMA decomposition was investigated as a first order reaction for most previous studies. PMMA ignites at 460°C and burns forming carbon dioxide, water, carbon monoxide and low molecular weight compounds, including formaldehyde. By following the temperature of the third endothermic peak listed in **Table 1(a)**, it is noticed that it increases for PMMA samples mixed with increasing the wt% of nano-TiO$_2$. This may be attributed to that as the content of nano-TiO$_2$ increases in the PMMA polymer; the composites became more thermally stable which indicate better dispersed of TiO$_2$ in PMMA matrix.

3.2. Differential Thermogravimety (DrTGA)

Differential thermogravimety (DrTGA) results of pure PMMA and those of mixed PMMA with different concentrations of nano-TiO$_2$ powder are shown in **Figure 2** and are listed in **Table 1**. From **Table 1**, the values of the decomposition temperatures for all the composites are detected. These decompositions depend upon the molecular weight and the purity of the polymer, *i.e.*, PMMA in this case, and are affected by its morphology. The second and third endothermic peaks for pure PMMA are detected at about 271.86°C and 325.00°C, respectively, which reflect the decomposed reaction of PMMA. The values of the second endothermic peak shifted toward lower temperatures by increasing the contents of TiO$_2$ and shows wide right shoulder as in the case of pure PMMA. This shoulder differs in depth according to the percentage content of nano-TiO$_2$. The appearance of the shoulder means that the average side of crystallites is changed due to the adding of nano-TiO$_2$ powder to PMMA
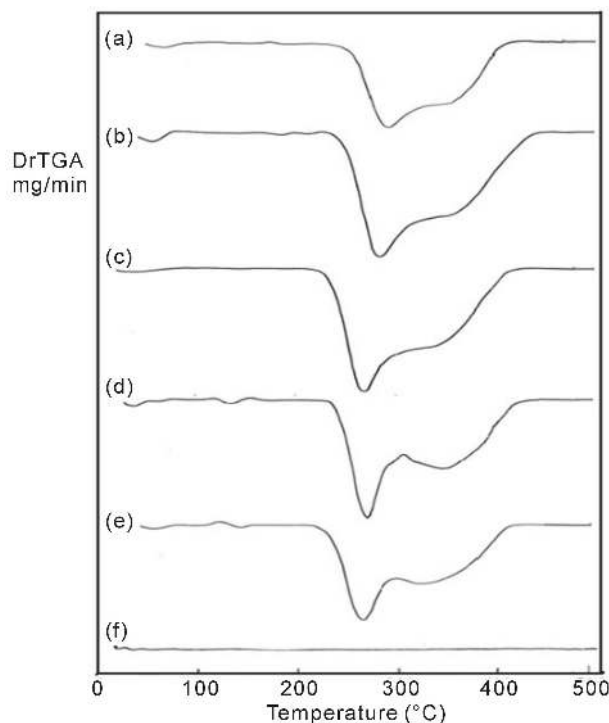
Figure 2. DrTGA curves of PMMA/TiO$_2$ nanoparticles composites: (a) 100/0, (b) 97.5/2.5, (c) 95/5, (d) 92.5/7.5, (e) 90/10 and (f) 0/100 (wt/wt%).

polymer. Heat release during the decomposition is represented at the end of the temperature curves for all composites which are assigned to the heat released of oxidation of the decomposition of flammable products of the samples.

3.3. Differential Scanning Calorimetry (DSC)

DSC is most commonly used to determine transition temperatures such as glass transitions, melting cross-linking reactions, purity and rate of decomposition. However, it measures only the total heat flow and the sum of all thermal transition in the sample and the rate of crystallization temperatures, in addition to the associated enthalpy for each process. Also, DSC has been used to measure heat of transition, specific heat, thermal emissivity and certain isothermal functions [32].

The thermal properties of PMMA/TiO$_2$ nanoparticles composites are examined by DSC to estimate how the thermal transitions of the prepared composites are affected by the presence of difference concentrations of TiO$_2$ and the data are shown in **Figure 3**. The measurements from the DSC curves are tabulated in **Table 2**. Difference in shape and area of the decomposition endothermic were noticed. From the figure and the table, the observed transitions can be assigned as follows [33] [34]:

The different in shape can be attributed to the different degree of crystallinity found in the different PMMA investigated samples. The broad endothermic peak observed around 44°C - 52°C indicted as O-H content declined. The hydroxyl groups are highly interconnected by hydrogen bonding, leads to higher glass transition temperature (T$_g$). The introduction of other functional groups (as nano-TiO$_2$ in our case) may support this bonding and enhance the T$_g$ value. Also, a reduction in the peak area indicated a change in the extent of crystallinity or in molecules order [35]. On the other hand, a decrease in enthalpy of fusion and increase in melting temperature suggested that the crystallinity and perfection of the crystal structure were reduced by increasing the degree of cross-linking. Change in the crystalline structure can results from PMMA polymer and earth metals molecules interactions in the amorphous phase of PMMA polymer. So, disorder in the crystals is created, reducing the enthalpy of the phase change [36] [37].

From **Figure 3** and **Table 2**, the major endothermic peaks are observed at 271.95°C and 362.85°C corre-
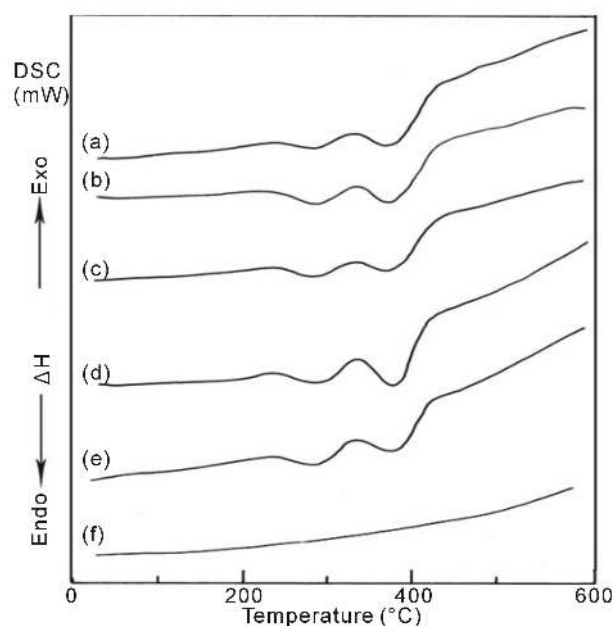
Figure 3. DSC curves of PMMA/TiO$_2$ nanoparticles composites: (a) 100/0, (b) 97.5/2.5, (c) 95/5, (d) 92.5/7.5, (e) 90/10 and (f) 0/100 (wt/wt%).

Table 2. Values of transition temperatures and associated heat of fusion for PMMA/TiO$_2$ nanoparticles composites.

PMMA/TiO$_2$ (wt/wt%)	Second step		Third step		Fourth step	
	Peak temperature (°C)	Heat release (J/g)	Peak temperature (°C)	Heat release (J/g)	Peak temperature (°C)	Heat release (J/g)
100/0	271.95	−36.83	326.17	15.36	362.85	−46.85
97.5/2.5	277.72	−53.00	327.48	11.23	367.20	−95.02
95/5	276.98	−33.51	327.85	16.52	364.06	−85.05
92.5/7.5	288.62	−33.00	323.32	17.21	372.01	−75.11
90/10	271.51	−82.25	331.05	15.5	368.76	−133.81
0/100	96.28	−1.43	191.70	−0.51		

sponding to the decomposition temperatures of the blank PMMA sample. For the other PMMA polymer mixed with TiO$_2$, the decomposition endotherms were slightly broadened and the peak temperature shifts towards higher values with increasing the concentration of TiO$_2$. Another exothermic peak is detected at 326.17°C corresponding to the decomposition temperature of the blank PMMA sample and the peak temperature slightly shifts towards higher values with increasing the concentration of TiO$_2$ up to 10 wt%.

It is noticed from **Table 2** that, the values of the heat of fusion (heat release, J/g), which is represented by the area under the endothermic and exothermic peaks of decomposition steps and its rate, has been found to be very effective to evaluate fire hazards. It can be detected that for the second step, PMMA/TiO$_2$ nanoparticles composite of 90/10 wt/wt% has the highest heat release value (−82.25 J/g) while composite of 92.5/7.5 wt/wt% has the lowest one (−33.00 J/g). For the third exothermic step, the highest heat release value is that for the composite 92.5/7.2 wt/wt% while the lowest one is that for the composite of 97.5/2.5 wt/wt%. In addition, the highest and lowest values of the heat release are those for the composites 90/10 and 100/0, respectively.

The decomposition temperature of any polymer depends on its molecular weight and its purity; also, it is affected by its morphology. This decomposition temperature depends on the crystallinity of the polymer—the highest the crystallinity has the higher decomposition peak [38]. The obtained changes in heat of fusion (J/g) and increase in the melting temperature points (T$_m$) suggested that the crystallinity and perfection of crystal structure are reduced with increasing of cross-linking. As well known by previously reported work [38], a change in the crystalline structure may result from polymer-filler interactions in the amorphous phase, therefore,

disorder in the crystals is created, reducing the enthalpy of the phase change. However, PMMA/TiO$_2$ nanoparticles composites show all the parent endotherms and exotherms with only a slight perturbation in the character of each component by degradation. Especially, the exotherm corresponding to combustion of the char residue seems to change with the additive ratio. Exothermic activity in composites occurs following melting, followed by a rise in the curve at about 327°C. This exotherm, which is nonoxidative in character, appears to play an important role in the formation of structure features to retard the flammability, by reactions such as dehydration and cross-linking [39] and also may be due to oxidative decomposition of a small amount of the residue that is formed during the first degradation correspond to dissociation of the methyl groups present in PMMA polymer. Around 440°C, a large exotherm appears in the thermogram of all the composites under investigation due to oxidative reactions of the polymer and combustion of the char residue [40]. Moreover, it is indicated from the obtained results that the addition of TiO$_2$ to PMMA enhances their thermal stability which is in agreement with previously reported work by Osiris *et al.* [23]

3.4. X-Ray Diffraction (XRD) Analysis

X-ray diffraction (XRD) analysis is used by many investigators to characterize the change in the crystal structure parameters such as: the degree of crystal orientation, the apparent crystal size and the lattice strain along the axis of the crystal unit cell [41]. XRD is used to check the crystalline formations of PMMA/TiO$_2$ nanoparticles composites. Their typical XRD patterns at room temperature in the scanning range $5 \leq 2\theta \leq 60°$ are represented in **Figure 4**. The appearance of sharp reflections and diffuse scattering observed from the XRD pattern of pure PMMA (pattern a), its characteristic of crystalline and amorphous phases of conventional semi-crystalline polymers. Moreover, this pattern shows several distinct crystallite peakss at $2\theta = 6.65$, 8.69 and 12.58 degrees. Most of these peaks are no longer detectable, since they are of vanishingly small intensity in the XRD patterns of the PMMA/TiO$_2$ composites. This is attributed to weak reflections from the ordered structure. In addition, from the patterns (b-f), it is noticed that, two new peaks started to appear at $2\theta = 27.42$ and 54.26 degrees for the composite 97.5/2.5 wt/wt% (pattern b). As the concentration (wt%) of nano-TiO$_2$ increased, these two peaks started growing and became as the major peakss in the largely composites and four other peaks are appeared at $2\theta = 25.27$ - 25.43, 36.01 - 36.22, 41.16 - 41.34 and 56.58 - 56.78 degrees (patterns c-e). These 6-appearance peaks indicate that the presence of TiO$_2$ with different weight percents can cause structural variation in the polymeric network of PMMA and also the baseline is heaved because of the existence of PMMA which is consistent with the previous results of FTIR [41]. The obtained peaks are observed to coincide with that present in the XRD pattern for pure nano-TiO$_2$ powder (pattern f) and confirm the presence of nano-TiO$_2$ crystallites within the polymeric matrix [42]. In **Figure 4**, the XRD pattern-f exhibited strong diffraction peaks at $2\theta = 25.43$, 27.56, 36.22, 41.34, 54.43 and 56.78 degrees indicating TiO$_2$ in the rutile and anatase phases [43]. All peaks are in good agreement with the standard spectrum (JCPDS no.: 88 - 1175 and 84 - 1286). Also, from the pattern f, it is shown the baseline is heaved because of the existence of the nano-TiO$_2$ powder which is composed of irregular polycrystalline. Amorphous revealed a broad pattern; however, the effect of the amorphous materials on the broadening of the XRD patterns of nanosized TiO$_2$ is negligible.

By following all of the peaks intensities at the different 2θ values (**Figure 4**), changes in the intensity of the XRD peaks of the composites are illustrated in **Figure 5**. It is noticed that the peaks intensities increased continuously with increasing nano-TiO$_2$ content up to 100 wt%. It must be noticed that the intensities of the peaks for all composites do not reach the intensities of the pure nano-TiO$_2$ peaks.

Two distinguished bands are centered at $2\theta = 13.5°$ - 14.8° and 30.0° - 31.0° as fundamental and secondary bands, respectively. **Table 3** illustrates the positions (2θ) and intensities of the fundamental (I_f) and secondary (I_s) bands as well as half-band-width (hbw) values calculated from the data of the X-ray patterns of PMMA/TiO$_2$ nanoparticles composites at the fundamental band and their percentage changes. It is clear from the table that a remarkable decrease in the half-band-width is observed for the composite 92.5/7.5 wt/wt%, which meant that crystallite size became larger (an inverse relation) [42].

Crystallinity is defined as the weight fraction of the crystalline portion of a polymer. The physical and mechanical properties of polymers are considerably dependent on that parameter. XRD is most frequently used to measure the crystallinity in the polymers. The method is based on the assumption that it is possible to separate the intensity contributions arising from the crystalline and amorphous regions. The degree of crystallinity is the ratio of the integrated intensity under the crystalline bands to the integrated intensity under the complete XRD
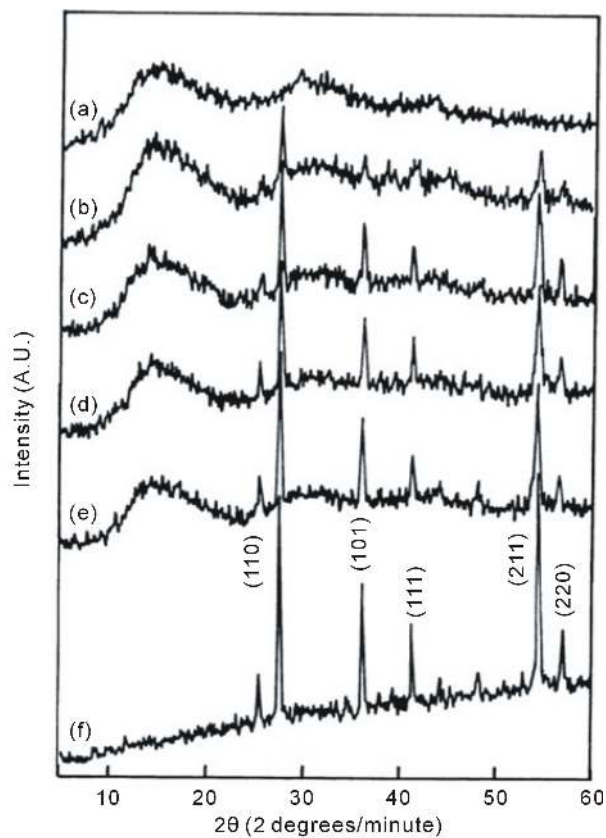
Figure 4. Variation in X-ray diffraction patterns of PMMA/TiO$_2$ nanoparticles composites: (a) 100/0, (b) 97.5/2.5, (c) 95/5, (d) 92.5/7.5, (e) 90/10 and (f) 0/100 (wt/wt%).
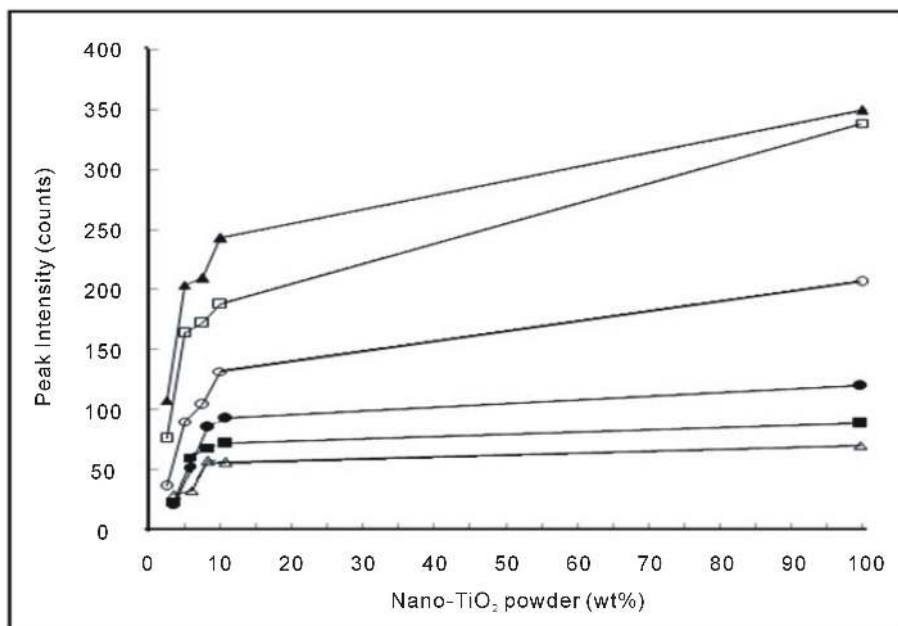

Figure 5. Variation of peaks intensity of XRD patterns at different angles for PMMA/TiO$_2$ nanoparticles composites: at 2θ: ($\triangle$) 25.27 - 25.43, ($\blacktriangle$) 27.39 - 27.56, (o) 36.01 - 36.22, ($\bullet$) 41.16 - 41.34, ($\square$) 54.23 - 54.43 and ($\blacksquare$) 56.58 - 56.78 degrees.

Table 3. 2θ, I_f, I_s, hbw and CrI as well as their percentage changes for PMMA/TiO$_2$ nanoparticles composites.

PMMA/TiO$_2$ (wt/wt%)	Fundamental band			Secondary band			hbf (deg.)	Δhbw%	CrI	% ΔCrI
	2θ (deg.)	I_f (AU)	% ΔI_f	2θ (deg.)	I_s (AU)	% ΔI_s				
100/0	14.8	33	-	30.0	29	-	1.8	-	12.12	-
97.5/2.5	14.5	43	30.3	31.0	36	24.1	2.1	16.7	16.28	34.3
95/5	13.5	37	12.1	31.0	30	3.4	1.8	0.0	18.92	56.1
92.5/7.5	14.8	33	0.0	30.2	28	−3.4	1.7	−5.6	15.15	25.0
90/10	14.8	29	−12.1	30.4	26	−10.3	1.9	5.6	10.34	−14.7
0/100	-	-	-	-	-	-	-	-	-	-

trace. Other measures, such as bands height may be used. With proper attention to experimental detail, this method provides one of the fundamental measures of crystallinity in polymers.

Table 3, also, represents the variation of crystallinity index (CrI) PMMA/TiO$_2$ nanoparticles composites as calculated from the X-ray patterns (**Figure 4**) by using Equation (1). It is clear from the table that, CrI values increase steeply, reaching a maximum value for the composite 95/5 wt/wt% and then decrease with increasing the content of nano-TiO$_2$. The increase in CrI may indicate that there was an increase in crystalline regions, whereas its decrease meant that amorphosity dominated. This implies changes in the structural regularity of the main chains of the polymeric molecules. The results indicate that structural changes occurred in the polymer matrix as the nano-TiO$_2$ diffused. The oxygen ions of TiO$_2$ were coordinated with the hydroxyl groups belonging to the different chains in PMMA. A decrease in crystallinity index has been proposed as one or another aspect of the complicated molecular and crystalline structure induced in mixing with nano-TiO$_2$ powder. It has been recognized that the nano-TiO$_2$ concentration plays a dominant role in both morphological and microstructural change in the polvmer matrix [42]. This may have been attributed to variations in the internal mechanisms that occurred by the induced effect of nano-TiO$_2$ on the structure of PMMA. As a result, it produced variations in the macromolecular and micromolecular structure of the PMMA network.

4. Conclusions

In the present work thermal methods such as thermal gravimetric analysis (TGA) and differential scanning calorimetry (DSC) are employed to study the change in the thermal stability of the PMMA/TiO$_2$ nanoparticles composites under investigation. From the obtained results an insight in understanding the structural changes occurring when PMMA is mixed with different weight percent of nano-TiO$_2$ is reported. Regarding the PMMA decompositions, the shift of the thermal peaks to higher temperature than that for pure PMMA can be explained assuming that the composites have better thermal stability due to the presence of nano-TiO$_2$. The increase in char yield with the increase of weight percentage of added nano-TiO$_2$ may be because PMMA main chains on the surface and inside the pores are more difficult to decompose than the pure PMMA which indicates that TiO$_2$ nanoparticle dispersion in PMMA matrix is uniform and thus hindered the segmental motion of PMMA chains. Therefore, the observed thermal analyses data contain information related to the structural properties of different materials and can be used to predict properties that are directly related to their physical performance as well as their thermal degradation parameters.

On the other hand, X-ray diffraction (XRD) analyses showed the sharpening of peaks at different nano-TiO$_2$ concentrations which confirmed changes in the crystallinity/amorphosity ratio and crystallite size. Moreover, the analyses of XRD revealed that the changes in crystallinity index with increasing the weight percent of TiO$_2$ confirmed the data obtained by using thermal (TGA and DSC) techniques.

References

[1] Burda, C., Chen, X., Narayanan, R. and El-Sayed, M.A. (2005) The Chemistry and Properties of Nanocrystals of Different Shapes. *Chemical Reviews*, **105**, 1025-1102. http://dx.doi.org/10.1021/cr030063a

[2] Yin, Y. and Alivisatos, A.P. (2005) Colloidal Nanocrystal Synthesis and the Organic-Inorganic Interface. *Nature*, **437**, 664-670. http://dx.doi.org/10.1038/nature04165

[3] Rothon, R.N. (2002) Particulate Fillers for Polymers. Rapa Review Reports Summary, 1st Edition.

[4] Ozkaraoglu, E., Tunc, I. and Suzer, S. (2009) Preparation of Au and Au-Pt Nanoparticles within PMMA Matrix Using

UV and X-Ray Irradiation. *Polymer*, **50**, 462-466. http://dx.doi.org/10.1016/j.polymer.2008.12.008

[5] Choudhary, B., Chawla, S., Jayanthi, K., Sood, K.N. and Singh, S. (2010) The Effect of Al and B on the Luminescent Property of Porous Silicon. *Current Applied Physics*, **10**, 807-812. http://dx.doi.org/10.1016/j.cap.2009.09.019

[6] Khanna, P.K., Singh, N. and Charan, S. (2007) Synthesis of Nanoparticles of Anatase TiO_2 and Preparation of Its Optical Transparent Film in PVA. *Materials Letters*, **61**, 47254730. http://dx.doi.org/10.1016/j.matlet.2007.03.064

[7] Singh, A., Kulkarni, U.K. and Khan-Malek, C. (2011) Patterning of SiO_2 Nanoparticle-PMMA Polymer Composite Microstructures Based on Soft Lithographic Techniques. *Microelectronic Engineering*, **88**, 939-944. http://dx.doi.org/10.1016/j.mee.2010.12.026

[8] Matsuyama, K. and Mishima, K. (2009) Preparation of Poly(methyl methacrylate)-TiO_2 Nanoparticle Composites by Pseudo-Dispersion Polymerization of Methyl Methacrylate in Supercritical CO_2. *Journal of Supercritical Fluids*, **9,** 256-264. http://dx.doi.org/10.1016/j.supflu.2009.03.001

[9] Lai, J.C.K., Lai, M.B., Jandhyam, S., Dukhande, V.V., Bhushan, A., Daniels, C.K. and Leungg, S.W. (2008) Exposure to Titanium Dioxide and Other Metallic Oxide Nanoparticles Induces Cytotoxicity on Human Neural Cells and Fibroblasts. *International Journal of Nanomedicine*, **3**, 533-545.

[10] Silva, A., Dahmouche, K. and Soares, B. (2010) The Effect of Addition *of* Acrylic Acid and Thioglycolic Acid on the Nanostructure and Thermal Stability of PMMA Montmorillonite Nanocomposites. *Applied Clay Science*, **47**, 414-420. http://dx.doi.org/10.1016/j.clay.2009.12.010

[11] Ma, W., Zhang, J., Wang, X. and Wang, S. (2007) Effect of PMMA on Crystallization Behavior and Hydrophilicity of Poly(vinylidene fluoride)/Poly(methyl methacrylate) Blend Prepared in Semi-Dilute Solutions. *Applied Surface Science*, **253**, 8377-8388. http://dx.doi.org/10.1016/j.apsusc.2007.04.001

[12] Wochnowski, C., Metev, S. and Sepold, G. (2000) UV—Laser-Assisted Modification of the Optical Properties of Polymethylmethacrylate. *Applied Surface Science*, **154-155**, 706-711. http://dx.doi.org/10.1016/S0169-4332(99)00435-3

[13] Schade, V.L. and Roukis, T.S. (2010) The Role of Polymethylmethacrylate Antibiotic-Loaded Cement in Addition to Debridement for the Treatment of Soft Tissue and Osseous Infections of the Foot and Ankle. *Journal of Foot and Ankle Surgery*, **49**, 55-62. http://dx.doi.org/10.1053/j.jfas.2009.06.010

[14] Mohanty, S.P., Kumar, M.N. and Murthy, N.S. (2003) Use of Antibiotic-Loaded Polymethyl Methacrylate Beads in the Management of Musculoskeletal Sepsis—A Retrospective Study. *Journal of Orthopaedic Surgery*, **11**, 73-79.

[15] Pleshko, N.L., Boskey, A.L. and Mendelsohn, R. (1992) An Infrared Study of the Interaction of Polymethyl Methacrylate with the Protein and Mineral Components of Bone. *Journal of Histochemistry and Cytochemistry*, **40**, 1413-1417. http://dx.doi.org/10.1177/40.9.1506677

[16] Stevens, A. and Germain, J. (1990) Resin Embedding Media. In: Bancroft, J.D. and Stevens, A., Eds., *The Theory and Practice of Histological Techniques*, 3rd Edition, Churchill Livingstone, New York.

[17] Chen, X. and Mao, S.S. (2007) Titanium Dioxide Nanomaterials: Synthesis, Properties, Modifications, and Applications. *Chemical Reviews*, **107**, 2891-2959. http://dx.doi.org/10.1021/cr0500535

[18] Millis, A. and Le Hunte, S. (1997) An Overview of Semiconductor Photocatalysis. *Journal of Photochemistry and Photobiology A*, **108**, 1-35. http://dx.doi.org/10.1016/S1010-6030(97)00118-4

[19] Fujishima, A., Rao, T.N. and Tryk, D.A. (2000) Titanium Dioxide Photocatalysis. *Journal of Photochemistry and Photobiology C*: *Photochemistry Reviews*, **1**, 1-21. http://dx.doi.org/10.1016/S1389-5567(00)00002-2

[20] Khaled, S.M., Sui, R., Charpentier, P.A. and Rizkalla, A.S. (2007) Synthesis of TiO_2-PMMA Nanocomposite: Using Methacrylic Acid as a Coupling Agent. *Langmuir*, **23**, 3988-3995. http://dx.doi.org/10.1021/la062879n

[21] Chen, W.C., Lee, S.J., Lee, L.H. and Lin, J.L. (1999) Synthesis and Characterization of Trialkoxysilane-Capped Poly-(methyl methacrylate)-Titania Hybrid Optical Thin Films. *Journal of Materials* Chemistry, **9**, 2999-3003. http://dx.doi.org/10.1039/a906157f

[22] Convertino, A., Leo, G., Striccoli, M., Di Marco, G. and Curri, M.L. (2008) Effect of Shape and Surface Chemistry of TiO_2 Colloidal Nanocrystals on the Organic Vapor Absorption Capacity of TiO_2/PMMA Composite. *Polymer*, **49**, 5526-5532. http://dx.doi.org/10.1016/j.polymer.2008.09.069

[23] Osiris, W.G., Mohamed, S.M. and El-Zaher, N.A. (2013) Macrostructure and Optical Study of PMMA/TiO_2 Nanopartcles Composites. *Nano Science and Nano Technology* (*An Indian Journal*), **7**, 60-65.

[24] Segal, L., Creely, J.J., Martin Jr., A.E. and Conrad, C.M. (1959) An Empirical Method for Estimating the Degree of Crystallinity of Native Cellulose Using the X-Ray Diffractometer. *Textile Research Journal*, **29**, 786-794. http://dx.doi.org/10.1177/004051755902901003

[25] Cao, J. and Bhoyro, A.Y. (2001) Structural Characterization of Wool by Thermal Mechanical Analysis of Yarns. *Textile Research Journal*, **71**, 63-66.

[26] Kim, J.H., Kim, J.Y., Lee, Y.M. and Kim, K.Y. (1982) Properties and Swelling Characteristics of Cross-Linked Poly(vinyl alcohol)/Chitosan Blend Membrane. *Journal of Applied Polymer Science*, **45**, 1711-1717. http://dx.doi.org/10.1002/app.1992.070451004

[27] Chiu, J. (1966) Applications of Thermogravimetry to the Study of High Polymers. *Applied Polymer Symposium*, **2**, 25-43.

[28] Peng, G.R., Li, Q.S., Yang, Y.L. and Wang, H.F. (2009) Degradation of Nano ZnO-Glass Fiber-Unsaturated Polyester Composites. *Journal of Applied Polymer Science*, **114**, 2128-2133. http://dx.doi.org/10.1002/app.29988

[29] Madras, G., Smith, J.M. and McCoy, B.J. (1996) Degradation of Poly(methyl methacrylate) in Solution. *Industrial & Engineering Chemistry Research*, **35**, 1795-1800. http://dx.doi.org/10.1021/ie960018b

[30] Costache, M.C., Heidecker, M.J., Manias, E. and Wilkie, C.A. (2006) The Thermal Degradation of PMMA Nanocomposites with Montmorillonite, Layered Double Hydroxides and Carbon Nanotubes. *Polymers for Advanced Technologies*, **17**, 272-280. http://dx.doi.org/10.1002/pat.697

[31] Holland, B.J. and Hay, J.N. (2001) The Kinetics and Mechanisms of the Thermal Degradation of Poly(methyl methacrylate) Studied by Thermal Analysis-Fourier Transform Infrared Spectroscopy. *Polymer*, **42**, 4825-4835. http://dx.doi.org/10.1016/S0032-3861(00)00923-X

[32] Osiris, W.G. and Moselhey, M.T.H. (2012) Thermal and Structural Studies of Poly(vinyl alcohol) and Hydroxypropyl Cellulose Blends. *Natural Science*, **4**, 57-67. http://dx.doi.org/10.4236/ns.2012.41009

[33] Abdelrazek, E.M., Elashmawi, I.S., El-Khodary, A. and Yassin, A. (2010) Structural, Optical, Thermal and Electrical Studies on PVA/PVP Blends Filled with Lithium Bromide. *Current Applied Physics*, **10**, 607-613. http://dx.doi.org/10.1016/j.cap.2009.08.005

[34] Pielichowski, K. and Njuguna, J. (2005) Thermal Degradation of Polymeric Materials. Smithers Rapra Technlogy.

[35] Ciemniecki, S.L. and Glasser, W.G. (1988) Multiphase Materials with Lignin: 1. Blends of Hydroxypropyl Lignin with Poly(methyl methacrylate). *Polymer*, **29**, 1021-1029. http://dx.doi.org/10.1016/0032-3861(88)90010-9

[36] Hammel, R., MacKnight, W.J. and Karasz, F.E. (1975) Structure and Properties of the System: Poly(2,6-dimethylphenylene oxide) Isotactic Polystyrene. Wide-Angle X-Ray Studies. *Journal of Applied Physics*, **46**, 4199-4203. http://dx.doi.org/10.1063/1.321432

[37] Wenig, W., Karasz, F.E. and MacKnight, W.J. (1975) Structure and Properties of the System: Poly(2,6-dimethylphenylene oxide) Isotactic Polystyrene. Small Angle X-Ray Studies. *Journal of Applied Physics*, **46**, 4194-4198. http://dx.doi.org/10.1063/1.321431

[38] Guan, J. and Chen, G. (2010) Copolymerization Modification of Silk Fabric with Organophosphorous Flame Retardant. *Fire and Materials*, **37**, 261-270.

[39] Fukatsu, K. (1993) Kinetic and Thermogravimetric Analysis of Thermal Degradation of Polychlal Fiber/Polyester Fiber Blend. *Journal of Applied Polymer and Science*, **47**, 2117-2123. http://dx.doi.org/10.1002/app.1993.070471205

[40] Langley, J.T., Drews, M.J. and Barker, R.H. (1980) Pyrolysis and Combustion of Cellulose. VII. Thermal Analysis of the Phosphorylation of Cellulose and Model Carbohydrates during Pyrolsis in the Presence of Aromatic Phosphates and Phosphoramides. *Journal of Applied Polymer Science*, **25**, 243-262. http://dx.doi.org/10.1002/app.1980.070250210

[41] Tortora, P. and Merkel, R. (2007) Fairchild's Dictionary of Textiles. 7th Edition, Fairchild's Book and Visuals, New York.

[42] El-Zaher, N.A. and Osiris, W.G. (2005) Thermal and Structural Properties of Poly(vinyl alcohol) Doped with Hydroxypropyl Cellulose. *Journal of Applied Polymer Science*, **96**, 1914-1923. http://dx.doi.org/10.1002/app.21628

[43] Thamaphat, K., Limsuwan, P. and Ngotawornchai, B. (2008) Phase Transition of TiO_2 Powder by XRD and TEM. *Kasetsart Journal* (*Natural Science*), **42**, 357-361.

Scientific Research Publishing (SCIRP) is one of the largest Open Access journal publishers. It is currently publishing more than 200 open access, online, peer-reviewed journals covering a wide range of academic disciplines. SCIRP serves the worldwide academic communities and contributes to the progress and application of science with its publication.

Other selected journals from SCIRP are listed as below. Submit your manuscript to us via either submit@scirp.org or Online Submission Portal.